Available online at www.sciencedirect.com
ScienceDirect
Ceramics International 36 (2010) 115–120
CERAMICS INTERNATIONAL
www.elsevier.com/locate/ceramint

Influence of fluorine content on the crystallization and microstructure of barium fluorphlogopite glass-ceramics

P.K. Maiti *, Amit Mallik, A. Basumajumdar, P. Kundu

Dept. of Chemical Technology (Ceramic Engineering Division), University of Calcutta, 92, Acharya Prafulla Chandra Road, Kolkata 700 009, India

Received 10 March 2009; received in revised form 18 March 2009; accepted 4 July 2009
Available online 11 August 2009

Abstract

The effect of varying the fluorine content on the nucleation and crystallization behavior of barium containing glasses based on the system $BaO{\cdot}4MgO{\cdot}Al_2O_3{\cdot}6SiO_2{\cdot}2MgF_2$ was investigated by differential thermal analysis (DTA), X-ray diffraction (XRD) and scanning electron microscopy (SEM).

Both the crystallization peak temperature (T_p) and activation energies (E) decreased, the Avrami exponent (n) and pre-exponential factor (ν) increased. The results suggest that fluorine increases the rate of diffusion in the glass and promotes initial crystallization in barium fluorphlogopite glasses.

Keywords: B. Microstructure-final; D. Glass; D. Glass-ceramics

1. Introduction

Machinable glass-ceramics, wherein two-dimensional mica crystals are nucleated internally and crystallized from fluorine-containing glasses have been developed [1–4] which can be machined to precise tolerances and surface finish with conventional metal working tools. The easy machinability of these glasses result from the unique microstructure of an interlocking plate-like mica crystals forming a 'house-of-cards' structure dispersed throughout a glassy matrix. During machining, fractures follow along the cleavage plane of the mica and glass matrix interfaces, and are repeatedly deflected, branched and blunted leading to a mere microscopic cracks. Existing commercial materials are based on potassium fluorphlogopite including Macor produced by Corning which are having very low strength. But glass-ceramics based on alkaline earth fluorphlogopites [5,7] and in particular barium fluorphlogopites are claimed to have two to three times higher strength than the corresponding potassium fluorphlogopite glass-ceramics [5].

Beall [1] undertook the first studies of the alkali earth fluormica glass-ceramics. Later on Hoda and Beall [5] investigated different glass compositions containing barium, calcium, and strontium close in composition to the respective fluorphlogopite stoichiometry. Most of the compositions were susceptible to crystallization during casting. Only a few stoichiometric compositions were investigated and despite offering improved mechanical and dielectric strength no further studies exist in the literature where compositional details are given.

Radonjic and Nikolic [6] studied the effect of different sources of fluorine as well as the concentration of it on the system based on $MgO–Al_2O_3–SiO_2$. They found different phases viz. fluoborite, norbergite and fluorphlogopite depending on the heat treatment temperature, fluorine source and concentration.

Uno [7] investigated glass-ceramics containing barium-mica in the system $Ba_{0.5}Mg_3(Si_3Al)O_{10}F_2–Mg_2Al_4Si_5O_{18}–Ca_3(PO_4)_2$. They found improved fracture toughness and bending strength values. Addition of tricalcium phosphate $Ca_3(PO_4)_2$ was claimed to improve the stability of the glasses prior to crystallization. But no specific compositional details were given. However, it was stated that the compositions were close to the $Ba_{0.5}Mg_3(Si_3Al)O_{10}F_2$ stochiometry.

Hu [8] studied the effect of fluorine on the crystallization and microstructure changes in the system $Li_2O–Al_2O_3–SiO_2$. They found that fluorine promotes initial crystallization and diffusion

* Corresponding author. Tel.: +91 9432889369; fax: +91 33 2351 9755.
E-mail address: prabir.maiti@gmail.com (P.K. Maiti).

0272-8842/$36.00
doi:10.1016/j.ceramint.2009.07.010

in the glass which results in lower crystallization temperature and also lower activation energy for crystallization.

Tian et al. [9] studied the effect of fluorine content on the crystallization of fluorsilicic mica glass and found that only $KMg_{3.25}Si_{3.625}O_{10}F_2$ crystallizes in the glass. They concluded that fluorine addition not only improves activation energy of crystal growth by enhancing the degree of irregularity of the interface between glass and crystal, but also increases the frequency factor by lowering the viscosity of glass.

Griggs et al. [10] studied devitrification and microstructural coarsening of a fluoride containing barium aluminosilicate glass. They reported that the fluorine-containing barium aluminosilicate glass crystallized rapidly at low processing temperatures relative to stoichiometric BAS glass.

But the effect of fluorine on the crystallization in barium fluorphlogopite glass-ceramics system has not previously been discussed. The purpose of this study is to characterize the crystallization kinetics and microstructure with the variation of fluorine content in the barium fluorphlogopite glass-ceramics.

2. Experimental

2.1. Glass preparation

For this study, glass batches have weight compositions of $BaCO_3$, SiO_2, $MgCO_3$, Al_2O_3 and MgF_2, given in Table 1. These materials were analytical grade reagents of high purity mostly from E. Merck. The three different glass batches were properly mixed in an attrition mill. The batches were melted in a platinum crucible in an electrically heated furnace, melt was kept at the maximum melting temperature of 1500 °C for 2 h for all the batches with occasional stirring with a platinum rod to homogenize the melt. The melts were poured in to a hot iron mould to make glass block of about 60 mm × 25 mm × 10 mm dimension. After releasing from the mould, the glass blocks were immediately transferred to an annealing furnace operating at about 650 °C and held for 1 h at the temperature followed by natural cooling to room temperature.

After annealing, the blocks were cut into pieces to about 2 mm thickness. These plates were fired at 720 °C for 2 h for nucleation. Subsequently heated to the corresponding crystallization temperature at a rate of 2 °C/min and the samples were kept at the crystallization temperature for 5 h.

2.2. Characterization techniques

2.2.1. Differential thermal analysis (DTA)

Differential thermal analysis (DTA) was done using Shimadzu DT40 thermal analyzer against α-alumina powder as reference material. The resulting glasses was crushed and finally ground to ∼75 μm suitable for DTA analysis. Non-isothermal experiments were performed by heating 17 mg sample, crystallized at different temperatures, at a heating rate of 5, 10, 15 and 20 °C/min. in the temperature range from ambient to 1000 °C. DTA was applied to calculate the activation energy by Kissinger equation and Avrami exponent by Augis–Bennet equation.

Table 1
Chemical composition of the glass batches (in g).

Batch	$BaCO_3$	$MgCO_3$	SiO_2	Al_2O_3	MgF_2	MgF_2 (% excess)
MA0	22.2	18.5	40.2	11.6	13.7	0.0
MA5	22.2	18.5	40.2	11.6	13.7	5.0
MA10	22.2	18.5	40.2	11.6	13.7	10.0

2.2.2. X-ray powder diffraction (XRD)

Six heat treatment temperatures for each batch were investigated by X-ray powder diffraction. All samples were heat treated using a heating rate of 10°/min to the nucleation temperature (720 °C), soaked for 2 h at this temperature, heated again at 2°/min to the corresponding crystallization temperature and was kept at the temperature for 5 h followed by natural cooling to room temperature. Samples from all the above mentioned glass were ground to ∼75 μm. XRD experiments were performed by X-ray powder diffractometer (PW 1830, Panalytical) using Ni filtered Cu Kα, X-radiation with a scanning speed of 2° (2θ) per minute. The diffraction pattern was recorded within Bragg angle range $10^\circ < 2\theta < 70^\circ$. The phases formed were identified by JCPDS numbers (ICDD – PDF2 data base).

2.2.3. Scanning electron microscopy (SEM)

Samples from all the crystallization temperature (heating schedule as mentioned earlier) were studied to investigate the microstructural development with back scattered electron imaging (BEI) mode in a scanning electron microscope, Hitachi, S3400N, Japan. Before analysis, surfaces were polished with 1 and 0.5 μm diamond pastes. The samples were etched chemically by HF solution for 15 s.

2.2.4. Density

The densities of all the samples, ceramised at different temperatures, were measured by water displacement method, following Archimedes principle.

3. Result and discussion

3.1. Results of differential thermal analysis

DTA curves for the three glass samples at a heating rate of 10 °C/min are shown in Fig. 1. Only one exothermic peak was observed in Batch-MA0. But with the increase in fluorine concentration, one additional peak is visible in MA10. The appearance of the additional peak might be due to the early crystallization of a phase rich in fluorine, probably MgF_2 in this case. This observation is similar to that of Hoda and Beall [5] in the high fluorine content alkaline earth mica glass-ceramics. We are considering the second peak for calculating activation energy and Avrami exponent for the Batch-MA10. The glass transition temperature (T_g) and glass crystallization peak temperature (T_p) shifted to lower temperature as the fluorine content increased. The observation is same as reported in a previous investigation [8].

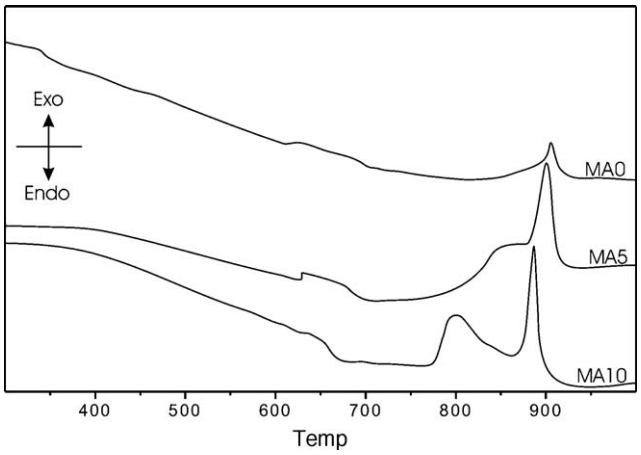

Fig. 1. Differential thermal analysis plots of glass samples with variation in Fluorine content. The rate of heating is 10 °C/min. (i) MA0 - 0% extra MgF_2, (ii) MA5 - 5% extra MgF_2 and (iii) MA10 - 10% extra MgF_2.

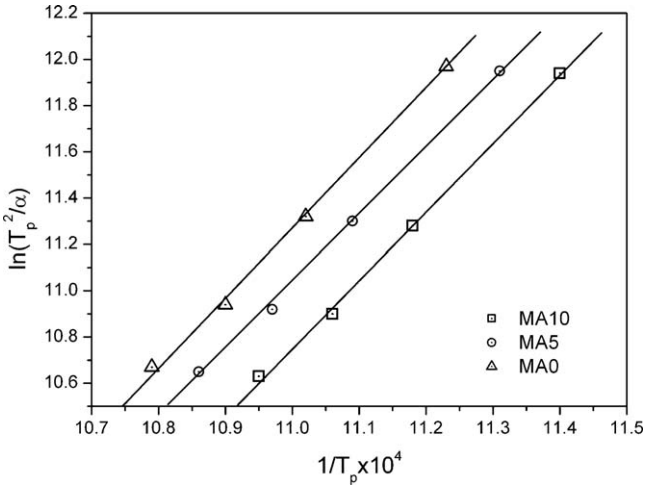

Fig. 2. Plots of $\ln(T_p^2/\alpha)$ vs. $1/T_p$ for different glass compositions.

From the Johnson–Mehl–Avrami (JMA) equation [12,13], non-isothermal crystallization kinetics of glass can be described by the Kissinger expression [14,15]

$$\ln\frac{T_p^2}{\alpha} = \frac{E}{RT_p} + \ln\frac{E}{R\nu}$$

where T_p is the crystallization peak maximum temperature in DTA curve, α is the heating rate, E is the activation energy and ν is the pre-exponential factor. T_p of samples of three batches at different heating rates are given in Table 2. From Table 2 we can see that T_p increased with increasing heating rate and decreased with increased fluorine content. Values of E and ν derived from the plots of $\ln(T_p^2/\alpha)$ versus $1/T_p$ in Fig. 2 are also given in Table 2. E decreased and ν increased with increasing fluorine.

Using the value of the activation energy, the Avrami exponent (n) was calculated by the Augis–Bennett equation [16]

$$n = 2.5\frac{RT_p^2}{\Delta TE}$$

where ΔT is the full width of the exothermic peak at the half-maximum intensity. The value of the Avrami exponent (n) is a parameter that is related to the crystallization mechanism.

According to JMA theory, the value of n being close to 2 means that surface crystallization dominates overall crystallization, while the value of 3 implies a two-dimensional and the value of 4 indicates a three-dimensional crystal growth for bulk materials [17–19].

From the above equation, the Avrami exponent gradually increased with increasing excess fluorine concentration in three different batches. The value was about 4, in this case, indicating that crystallization of the glass-ceramics was largely homogenous and assuming a three-dimensional pattern/character.

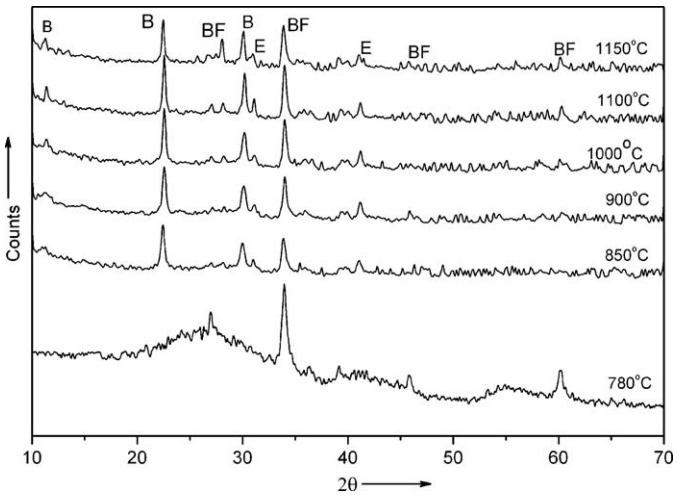

Fig. 3. XRD patterns for glass samples with no extra percentage of fluoride (MA0), ceramised at different temperatures for 5 h. B - barium aluminium silicate, BF - barium magnesium aluminium fluoride silicate and E - enstatite.

Table 3
List of JCPDS files used to identify the main crystal phase formed at different temperatures.

Crystal phase	JCPDS reference file
Barium fluorphlogopite ($BaMg_3Al_2Si_2O_{10}F_2$) – BF	00-019-0117
Barium aluminium silicate ($BaAl_2Si_2O_8$) – B	00-026-0137
Magnesium silicate (Enstatite) ($MgSiO_3$) – E	00-019-0768

Table 2
T_p (K), E and ν of the samples.

Batch	5 (K min^{-1})	10 (K min^{-1})	15 (K min^{-1})	20 (K min^{-1})	E (kJ mol^{-1})	ν (min^{-1})
MA0	890 ± 2	907 ± 2	917 ± 2	926 ± 2	248.3 ± 3	(7.2 ± 0.2) × 10^{13}
MA5	885 ± 2	901 ± 2	911 ± 2	920 ± 2	246.5 ± 3	(7.3 ± 0.2) × 10^{13}
MA10	877 ± 2	894 ± 2	904 ± 2	913 ± 2	244.8 ± 3	(7.4 ± 0.2) × 10^{13}

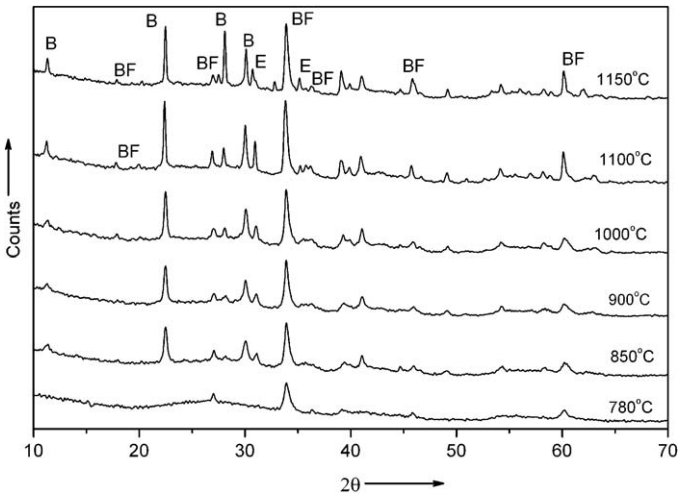

Fig. 4. XRD patterns for glass samples with 5% extra fluoride (MA5), ceramised at different temperatures for 5 h. B - barium aluminium silicate, BF - barium magnesium aluminium fluoride silicate and E - enstatite.

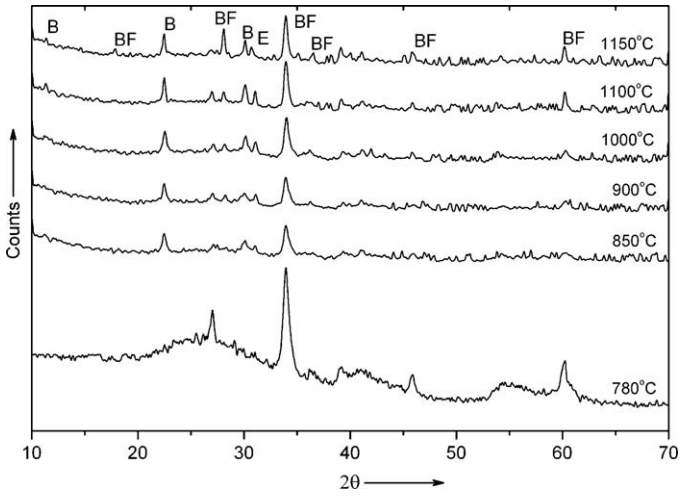

Fig. 5. XRD patterns for glass sample with 10% extra fluoride (MA10), ceramised at different temperatures for 5 h. B - barium aluminium silicate, BF - barium magnesium aluminium fluoride silicate and E - enstatite.

3.2. Results of X-ray diffraction

The JCPDS reference files used to identify the various crystal phases formed are presented in Table 3.

In all the heat treated samples of any particular batch, barium fluorphlogopite is observed as a major phase at lower heat treatment temperatures. This observation is similar to that of Beall [1] and Henry [11]. At 850 °C, peaks of enstatite and barium aluminium silicate appeared as new phase along with barium fluorphlogopite (BF). From 850 to 1000 °C there is no change in the intensity of the peaks and no new phases appeared, but a new peak of BF at 18° (2θ) appeared beyond 1000 °C which is visible only in the batches MA5 and MA10 (Figs. 3–5). But at 1100 and 1150 °C the sharpness of the peaks of both barium aluminium silicate and enstatite have been increased. It has also been observed that with increase in

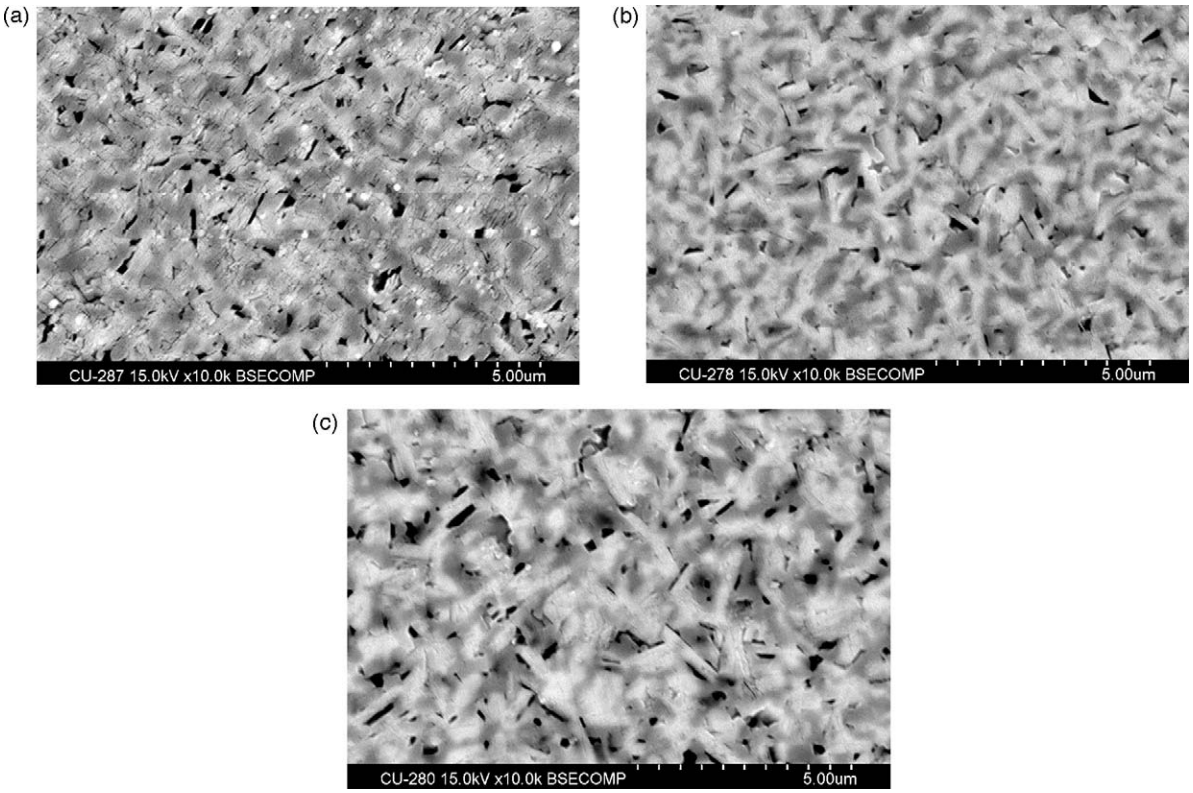

Fig. 6. (a) SEM photographs of polished and etched surface of MA0, nucleated at 720 °C for 2 h and ceramised at 1100 °C for 5 h. (b) SEM photographs of polished and etched surface of MA5, nucleated at 720 °C for 2 h and ceramised at 1100 °C for 5 h. (c) SEM photographs of polished and etched surface of MA10, nucleated at 720 °C for 2 h and ceramised at 1100 °C for 5 h.

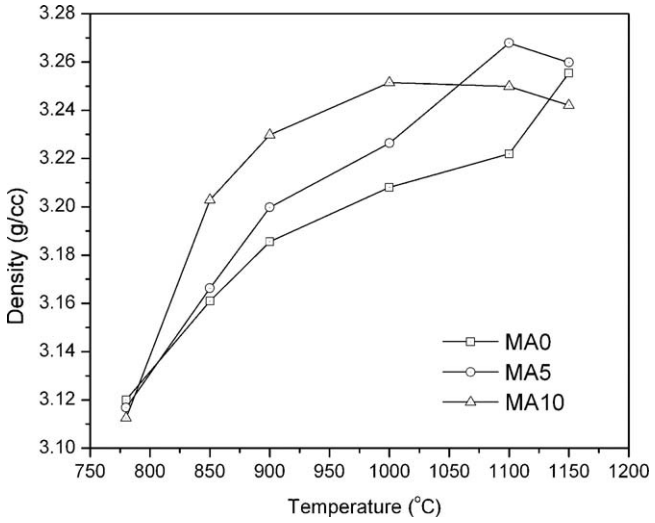

Fig. 7. Variation of bulk density with different ceramisation temperature (soaked for 5 h) of glass samples MA0, MA5, and MA10.

ceramisation temperature, the formation of barium aluminium silicate increases for any particular batch. With increase in fluorine content, the peaks at 11.31°, 22.5° and 30.09° (2θ), which is supposed to correspond to barium aluminium silicate have been reduced drastically. This may indicate that the excess fluorine reduces the chances of decomposition of BF into barium aluminium silicate.

3.3. Results of scanning electron microscopy

The microstructure of the three different batches of glass, having different fluorine content, ceramised at 1100 °C for 5 h are shown in Fig. 6a–c. Fig. 6a exhibited very fine microstructures consisting of small acicular barium fluorphlogopite crystals. Fig. 6b and c consists of large crystals of barium fluorphlogopite that are electron dense and appeared white in the backscattered electron images. It has also been observed that the sizes of the crystals increased with the increase in fluorine content. Some cracks have been observed at higher temperatures as well as with higher fluorine content. These findings suggest that fluorine promotes crystallization and growth.

3.4. Physical properties

Densities of as-prepared glasses were about 3.08–3.09 gm/cm^3. The density changes of the glass-ceramic heat treated at 780–1150 °C for 5 h are shown in Fig. 7 for three different batches. For Batch-MA0, density increases with increasing heat treatment temperature. But Batch-MA5 and Batch-MA10, density achieves the maximum value at 1100 °C, beyond this the density decreased with increasing heat treatment temperature. The decrease in density may be attributed to the decomposition of fluorphlogopite and propagation of cracks into interlocking mica crystals accompanied by crystal growth. This has been corroborated by the SEM observations. This observation suggests the ease of formation of BF at lower temperatures with increasing amount of fluorine. The findings are similar to the observations made by Radonjic [6].

4. Conclusions

The glass transition temperature (T_g) and glass crystallization peak temperature (T_p) shifted to lower temperatures as the fluorine content increased. The peak crystallization temperature was shown to correspond to the crystallization of barium fluorphlogopite. No other crystal phases were found prior or after the formation of barium fluorphlogopite, although the other phases viz. enstatite and BAS present in X-ray diffraction pattern seems to be very minor in the ceramised samples. From the calculation of Avrami exponent, these results indicated that crystallization of the glass was largely homogeneous. All these findings indicate that fluorine promotes initial crystallization.

Acknowledgements

The authors acknowledge the financial support extended by UPE scheme of University Grants Commission and also thankful for the XRD and SEM facility provided by the Technical Education Quality Improvement Programme.

References

[1] G.H. Beall, in: L.L. Hench, S.W. Frieman (Eds.), Advances Nucleation and Crystallization in Glasses, American Ceramic Society, Westerville, 1971, p. 251.
[2] D.G. Grossman, Machinable glass-ceramics based on tetrasilisic mica, J. Am. Ceram. Soc. 55 (1972) 446.
[3] C.K. Chyung, G.H. Beall, D.G. Grossman, Fluorphlogopite Mica Glass-Ceramics, in: Proceedings of the International Glass Congress No.14 Kyoto, Japan, Ceramic Society of Japan, Tokyo, Japan, (1974), pp. 33–40.
[4] G.A. Beal, C.K. Chyung, US Patent. 3,801,295.
[5] S.N. Hoda, G.H. Beall, in: J.H. Simmons, D.R. Ulhmann, G.H. Beall (Eds.), Alkaline Earth Mica Glass-Ceramics, Advances in Ceramics: Nucleation and Crystallization in Glasses, J. Am. Ceram. Soc. 2 (1982) 287.
[6] L.J. Radonjic, L.J. Nikolic, The effect of fluorine source and concentration on the crystallization of machinable glass-ceramics, J. Eur. Ceram. Soc. 7 (1991) 11–16.
[7] T. Uno, T. Kasuga, K. Nakjima, High-strength mica containing glass-ceramics, J. Am. Ceram. Soc. 74 (1991) 3139.
[8] A.-M. Hu, K.-M. Liang, F. Peng, G.-L. Wang, H. Shao, Crystallization and microstructure changes in fluorine-containing Li_2O–Al_2O_3–SiO_2 glasses, Thermochim. Acta 413 (1-2) (2004) 53–55.
[9] J. Tian, X. Cao, Y. Zhang, C. Wang, Effect of fluorine content on the crystallization of fluorsilicic mica glass, J. Mater. Sci. 37 (9) (2002) 1789–1792.
[10] J.A. Griggs, K.J. Anusavice, J.J. Mecholsky, Devitrification and microstructural coarsening of a fluoride-containing barium aluminosilicate glass, J. Mater. Sci. 37 (2002) 2017–2022.
[11] J. Henry, R.G. Hill, Influence of alumina content on the nucleation crystallization and microstructure of barium fluorphlogopite glass-ceramics based on $8SiO_2{\cdot}YAl_2O_34MgO2MgF_2BaO$ Part I Nucleation and crystallization behaviour, J. Mater. Sci. 39 (2004) 2499–2507.
[12] M. Avrami, Kinetics of phase change. 1. General theory, J. Chem. Phys. 9 (1939) 1103–1112.
[13] W.A. Johnson, K.F. Mehl, Trans. AIME 135 (1939) 416–442.

[14] H.E. Kissinger, Variation of peak temperature with heating rates in differential thermal analysis, J. Res. Natl. Bureau Stand. 57 (1956) 217–221.
[15] H.E. Kissinger, Reactions kinetics in differential thermal analysis, Anal. Chem. 29 (1957) 1702–1706.
[16] J.A. Augis, J.E. Bennett, Calculation of the Avrami parameters for heterogeneous solid state reactions using a modification of the Kissinger method, J. Therm. Anal. 13 (1978) 283–292.
[17] K. Cheng, Evaluation of crystallization kinetics of glasses by non-isothermal analysis, J. Mater. Sci. 36 (2001) 1043–1048.
[18] J.P. Young, H. Jong, Nucleation and crystallization kinetics of glass derived from incinerator fly ash waste, Ceram. Int. 28 (6) (2002) 669–673.
[19] L.A. Perez-Maqueda, J.M. Criado, J. Malek, Combined kinetic analysis for crystallization kinetics of non-crystalline solids, J. Non-Cryst. Solids 320 (1–3) (2003) 84–91.